

Libration points and periodic orbit families near a binary asteroid system with different shapes of the secondary

Ruikang Zhang^a, Yue Wang^{a,*}, Yu Shi^b, Shijie Xu^a

^a School of Astronautics, Beihang University, Beijing, 102206, China

^b Key Laboratory of Space Utilization, Technology and Engineering Center for Space Utilization, Chinese Academy of Sciences, Beijing, 100094, China

ARTICLE INFO

Keywords:

Binary asteroids
 Restricted full three-body problem
 Libration points
 Periodic orbit families
 Bifurcations
 Shape uncertainty

ABSTRACT

Due to the limited capability of ground-based observations, the shapes of asteroids cannot be determined precisely, especially for the secondary of a binary system. In this paper, libration points and periodic orbit families near a binary asteroid system with different shapes of the secondary are investigated, with the binary 66391 Moshup, previously known as 1999 KW4, as an example. The gravity fields of the primary and secondary of the binary system are modelled as those of a polyhedron and a triaxial ellipsoid, respectively. With a nominal shape model for the secondary, the positions and stability of libration points are determined, and periodic orbit families emanating from each libration point are generated by numerical methods. The connections and bifurcations of periodic orbit families are analyzed through comparisons with the classic results of the circular restricted three body problem (CR3BP). Then, the effect of the shape uncertainty is investigated by changing the shape of the secondary. Libration points and associated periodic orbit families are calculated and analyzed with different shapes of the secondary. It has been found that the libration points have slight offsets on position, but their topological structures remain the same. In some cases, the halo orbit family bifurcates from the vertical Lyapunov orbit family rather than the planar Lyapunov orbit family, indicating that bifurcations of periodic orbit families are different and new connections between periodic orbit families can exist. The results will provide general insights into variations of the dynamical environments near a binary asteroid system caused by different shapes of the secondary, and will be helpful for the planetary science research and exploration mission design.

1. Introduction

The study of dynamical environments near a binary asteroid system is of great interest for both the planetary science and exploration mission design. Since the first binary asteroid system 243 Ida was discovered by the Galileo spacecraft in 1993, quite a lot of binary asteroid systems have been discovered in the last few decades. It is currently estimated that up to 16% of the Near-Earth Asteroids (NEAs) and small ($D < 10$ km) main-belt asteroids (MBAs) are binaries (Margot et al., 2002) [1]. These small asteroid binaries are relatively uniform and typically contain a fast-spinning, spheroidal primary and a synchronously rotating, elongated secondary (Čuk and Nesvorný 2010) [2]. The study of dynamical environments near binary asteroid systems can provide important information about their formation and evolution. In recent years, several spacecraft have been delivered to explore asteroids, such as NEAR Shoemaker to 433 Eros, Hayabusa to 25143 Itokawa, Dawn to 4 Vesta, Hayabusa2 to 162173 Ryugu, and OSIRIS-REx to 101955 Bennu.

The binary asteroids have also been selected as the targets of exploration missions. For example, the Asteroid Impact and Deflection Assessment (AIDA) mission, which will be the first mission devoted to explore a binary asteroid system, 65803 Didymos, is currently under development at NASA and ESA. The unusual dynamical environments near binary asteroid systems are of fundamental importance for designing the spacecraft navigation and control.

Due to the irregular shapes of asteroids and the close distance between the primary and secondary, the dynamics of a massless body in the gravity field of a binary asteroid system is considered as the restricted full three body problem (RF3BP) (Scheeres and Bellerose, 2005) [3], which has a more complicated gravity field than the classic restricted three-body problem. In order to investigate the dynamical environments, the gravity fields of the asteroids need to be described by adequate models. By assuming that the asteroids are homogeneous, shape-based methods can be used to model the asteroid as an object with a specific shape, such as an ellipsoid (Scheeres, 1994) [4] or a

* Corresponding author.

E-mail addresses: zhangruikang@buaa.edu.cn (R. Zhang), ywang@buaa.edu.cn (Y. Wang), 93shiyu@gmail.com (Y. Shi), starsjxu@163.com (S. Xu).



Polyhedron (Werner and Scheeres, 1996) [5].

The ellipsoid model has been broadly used to investigate the dynamical environments in the vicinity of a binary asteroid system. Bellerose and Scheeres (2005, 2008a, 2008b) [6–8] have used the sphere-ellipsoid model to study the full two body problem (F2BP) and RF3BP with the binary system 66391 Moshup as an example. Chappaz and Howell (2015) [9] have used the ellipsoid-ellipsoid model to study bounded motions in both the synchronous and non-synchronous binary systems, including libration point orbits and resonant orbits. Woo and Misra (2015) [10] have investigated bounded trajectories near libration points by modeling the asteroids as an ellipsoid and a truncated ellipsoidal cone, which introduced asymmetry along the vertical direction. Hou et al. (2017) [11] have used the ellipsoid model to investigate locations and stability properties of the triangular equilibrium points in the double-ellipsoid systems of varying parameters, and demonstrated that the spherical harmonic method is problematic when identifying equilibrium points in close vicinity of the asteroids. Hou et al. (2017) [12] have used the ellipsoid model to verify the constructed first-order solutions to the rotational and orbital motion of the two bodies in the planar full two-body problem and solutions to the equations of motion (EOMs) for the related restricted full three-body problem. Li et al. (2017) [13] have investigated the equilibria points and their stabilities in the doubly-synchronous binary asteroid systems, which are modelled as two triaxial ellipsoids with various shapes and system parameters. Li et al. (2017) [14] have presented a novel method for the design and maintenance of a bounded trajectory near non-synchronized binary systems which are also modelled as two triaxial ellipsoids. However, the ellipsoid model cannot take into account the asymmetry of the gravity fields caused by the irregular shapes of asteroids. As a more accurate model, the polyhedron shape model was proposed by Werner and Scheeres (1996) [5]. Shi et al. (2018) [15] have used the polyhedron model for both the primary and secondary to study libration points and associated periodic orbit families in the synchronous and non-synchronous binary asteroid systems, with the binary 66391 Moshup as an example. Dell'Elce et al. (2017) [16] investigated the dynamical environments near the binary 65803 Didymos with a realistic RF3BP model by using the polyhedron-ellipsoid model, and they provided two safe orbits, the terminator and interior retrograde orbits. Capannolo et al. (2018) [17] have used the polyhedron-ellipsoid model to investigate families of bounded orbits near the binary asteroid 65803 Didymos.

Due to the limited capability of ground-based observations, the shape data of asteroids are difficult to obtain, and shape uncertainty always exists, especially for the secondary of a binary system. The effect of the shape uncertainty needs to be considered in the study of the dynamical environments. A few scholars have paid attention to this subject. Taking into account the different shapes of the primary and secondary, Woo and Misra (2014) [18] have investigated the variations of locations of the libration points about a binary asteroid system. However, more aspects of effects of the shape uncertainty on the dynamical environments still remain to be investigated.

As one of the most important dynamical structures of the three-body problem, libration point orbits are of great interest in study of dynamical environments near a binary asteroid system. Libration point orbits have been extensively studied in the circular restricted three-body problem (CR3BP). Numerical methods, such as those used by Gómez and Mondelo (2001) [19] and Koon et al. (2008) [20], can be well applied to RF3BP. Libration point orbits near a binary asteroid system have been studied by Bellerose and Scheeres (2008a) [7], Chappaz and Howell (2013, 2015) [21] [9], Shi et al. (2018) [15], and Capannolo et al. (2018) [17]. In particular, Shi et al. (2018) [15] pointed out that the bifurcations of the libration point orbits in RF3BP are different from those in the classical CR3BP, which was also discovered by Scheeres (2019) [22] in the Mars-Phobos system. Bifurcations of periodic orbit families are important properties of a dynamical system. Some studies have been devoted to the bifurcations of periodic orbit families around a single asteroid. Jiang et al. (2015) [23] divided the topological

structures of periodic orbits into 34 cases, and discussed tangent bifurcation, period-doubling bifurcation, Neimark–Sacker bifurcation, and real saddle bifurcation of the periodic orbits in the gravity field of an irregular-shaped body. Ni et al. (2016) [24] investigated the multiple bifurcations in periodic orbit families in the gravity field of the asteroid 433 Eros. However, the influence of shape uncertainty on the periodic orbits and their bifurcations have not been investigated yet, for a binary asteroid system, whose secondary usually has a higher shape uncertainty.

In this study, variations of libration points and associated periodic orbit families about a binary asteroid system caused by the shape uncertainty of the secondary will be investigated specifically. A suitable model for the gravity field of an irregular-shaped binary asteroid system is used, with the primary modelled as a homogeneous polyhedron and the secondary modelled as a homogeneous triaxial ellipsoid, as in Capannolo et al. (2018) [17]. The main reason for adopting the polyhedron-ellipsoid model rather than our previous polyhedron-polyhedron model in Shi et al. (2018) [15] is that the shape parameters of the triaxial ellipsoid can be easily changed to take into account the shape uncertainty of the secondary. The binary asteroid system 66391 Moshup is chosen as an example. The configuration and parameters of the binary system obtained from previous research are close to the real state of the binary system. Considering that small asteroid binaries typically contain a fast-spinning, spheroidal primary and a synchronously rotating, elongated secondary, we will consider the doubly-synchronous state for the binary system, as in previous studies, e.g., Refs. [7–11,13,15–18]. It is assumed that both the primary and secondary are rotating synchronously with their mutual orbital motion, which is justified because of the spheroidal shape of the primary. These assumptions cause some deficiencies in the dynamic model, but the results can still provide general insights into the dynamical environments in the proximity of small binary asteroids.

The doubly-synchronous assumption implies that the motion of the massless body is autonomous, as in the CR3BP. Thus, some methods used in the CR3BP can be applied well to our problem. With a nominal shape model for the secondary, the libration points in the gravity of the binary system will be calculated. By using homotopy and shooting methods, periodic orbits emanating from each libration point will be generated, and a pseudo-arclength continuation method will be used to facilitate the computation of periodic orbit families. Notably, the bifurcations of periodic orbits in the highly irregular gravity field will be analyzed through comparisons with the classic CR3BP to investigate effects of irregular shapes of the asteroids. Then, variations of libration points and associated periodic orbit families with different shapes of the secondary will be investigated. The shape of the secondary is varied by changing the semi-axes of the ellipsoid model with its mass unchanged in order to maintain the mass ratio of the binary system.

2. Background

In this section, equations of motion are constructed based on the RF3BP, numerical methods used for orbit family calculation are introduced, and the topological structures and bifurcations of periodic orbits are discussed.

2.1. Equations of motion

A massless particle moving in the gravity field of a binary asteroid system is considered, as shown in Fig. 1 M_1 and M_2 are the primary and secondary of the binary system, respectively. The motion of the primary and secondary are assumed to be circular around the barycenter of the binary system with a constant angular velocity ω . Because of the spheroidal shape of the primary, the fast spin of the primary is ignored, and then both the primary and secondary are rotating synchronously with their mutual orbital motion, implying that both the primary and secondary are stationary in the synodic frame. The synodic frame has its

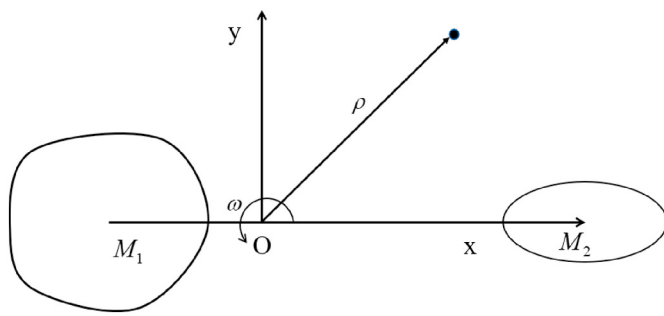


Fig. 1. A massless particle moving in the gravity field of a binary asteroid system.

origin in the barycenter of the binary system, with the x -axis pointing towards the barycenter of secondary, the z -axis aligned along angular momentum of the system, and the y -axis satisfying the right-handed basis. The position vector of the particle in the synodic frame is denoted by ρ .

The primary is modelled as a homogeneous polyhedron, and the secondary is modelled as a homogeneous triaxial ellipsoid. The equations of motion of the particle expressed in the synodic frame are (Belcerose and Scheeres 2008b) [8].

$$\begin{aligned}\ddot{x} - \omega^2 x - 2\omega\dot{y} &= U_{poly_x} + U_{ell_x}, \\ \ddot{y} - \omega^2 y + 2\omega\dot{x} &= U_{poly_y} + U_{ell_y}, \\ \ddot{z} &= U_{poly_z} + U_{ell_z},\end{aligned}\quad (1)$$

where x , y , and z represent components of the position of the particle in the synodic frame, U_{poly} and U_{ell} are the force potential (the negative of the gravitational potential) of the particle by the primary and secondary, respectively, and the subscripts x , y , and z indicate partial derivatives of the force potential.

The equations of motion can be rewritten in a vector form as:

$$\dot{X} = f(X), \quad (2)$$

where $X = [x, y, z, \dot{x}, \dot{y}, \dot{z}]^T$ and

$$f(X) = \begin{bmatrix} \dot{x} \\ \dot{y} \\ \dot{z} \\ \omega^2 x + 2\omega\dot{y} + U_{poly_x} + U_{ell_x} \\ \omega^2 y - 2\omega\dot{x} + U_{poly_y} + U_{ell_y} \\ U_{poly_z} + U_{ell_z} \end{bmatrix} \quad (3)$$

The force potential of the particle by the primary in the body-fixed frame is (Werner and Scheeres 1996) [5].

$$U_{poly} = \frac{1}{2} G \sigma \left(\sum_{e \in \text{edges}} L_e r_e^T E_e r_e - \sum_{f \in \text{faces}} \omega_f r_f^T F_f r_f \right), \quad (4)$$

where G is the gravitational constant, σ represents the primary's bulk density, r_e and r_f are body-fixed vectors from the particle to the edge e and the face f , respectively, E_e and F_f are geometric parameters of the edges and faces, respectively, L_e is an integration factor of the particle's position and the edge e , and ω_f is the solid angle of the face f relative to the particle.

The force potential of the particle by the secondary in the body-fixed frame is (Danby, 1992) [25].

$$U_{ell} = \frac{3}{4} G m_2 \int_{\lambda}^{+\infty} \varphi(r, v) \frac{dv}{\Delta(v)}, \quad (5)$$

with

$$\varphi(r, v) = 1 - \frac{x^2}{\alpha^2 + v} - \frac{y^2}{\beta^2 + v} - \frac{z^2}{\gamma^2 + v}, \quad (6)$$

$$\Delta(v) = \sqrt{(\alpha^2 + v)(\beta^2 + v)(\gamma^2 + v)}, \quad (7)$$

where m_2 denotes the mass of the secondary, α , β , and γ are the semi-axes of the ellipsoid, which satisfy $\alpha \geq \beta \geq \gamma > 0$, and the parameter λ satisfies $\varphi(r, \lambda) = 0$.

2.2. Numerical methods

Many numerical methods applied for calculating periodic orbit in CR3BP can also be applied to calculate periodic orbits in our RF3BP. However, the polyhedron model of the primary causes a much higher computational cost. Therefore, effective numerical methods are needed to save computational time. In our study, generally there are three steps to generate periodic orbit families.

First, we need to find an initial guess for a periodic orbit. The initial guesses of Lyapunov orbits can be easily found by adjusting the velocity magnitude with the bisection method thanks to their near planarity. However, the bisection method cannot effectively find initial guesses for spatial periodic orbits, such as the halo orbits and the axial orbits. Thus, the homotopy method will be used as a bridge between our RF3BP and the classical CR3BP, to provide the initial guesses for spatial periodic orbits in the RF3BP based on the classical results in the CR3BP. In the homotopy method, a fictitious gravity field $\varepsilon U_{RF3BP} + (1-\varepsilon) U_{CR3BP}$ is constructed, where ε is the homotopy parameter, and U_{CR3BP} and U_{RF3BP} represent the force potential of the CR3BP and RF3BP, respectively. By gradually increasing the homotopy parameter ε from 0 to 1, the periodic orbits in CR3BP can be finally corrected to the periodic orbits in RF3BP.

Then, the initial guess will be corrected to finally get a periodic orbit by the multiple shooting method, which has been commonly used in the CR3BP. In the multiple shooting method, the orbit is divided into several segments, and then each segment is integrated independently and corrected to satisfy constraints. Integrating each segment rather than the whole orbit can significantly reduce the sensitivity of orbits and achieve better convergence.

Finally, the periodic orbit family will be obtained by using the continuation method. There are two kinds of continuation methods commonly used in the CR3BP, the single-parameter continuation method and the pseudo-arclength continuation method. In the typical single-parameter continuation method, the direction of continuation depends on a physical quantity, such as the period or energy of the orbit, whereas in the pseudo-arclength continuation method, the direction of continuation is constructed to be tangent to the orbit family, guaranteed to be toward the next expected orbit. In this study, the pseudo-arclength continuation method will be adopted, and the direction of continuation will be determined based on two parameters of the orbit to ensure that the whole orbit family can be obtained. The period and a characteristic quantity of the orbit, such as the y -amplitude for the Lyapunov orbit and the z -amplitude for the halo orbit, are each selected to be the criterion of the continuation direction. This method can provide a better initial guess for the next orbit than the typical single-parameter continuation method, and, then, can reduce the iterations of the multiple shooting method.

2.3. Topological structures and bifurcations of periodic orbits

After the periodic orbit families are obtained, their topological structures and bifurcations can be analyzed. Eigenvalues of the monodromy matrix, called characteristic multipliers, determine the topological structure of the periodic orbit. The monodromy matrix M of the periodic orbit is defined as

$$M = \Phi(T) = \int_0^T A(\tau) d\tau, \quad (8)$$

where T denotes the period of the orbit, $\Phi(t)$ is the state transition

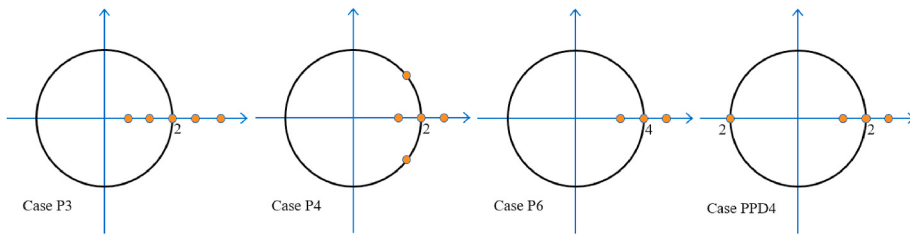


Fig. 2. Four cases of topological structures of libration orbit families.

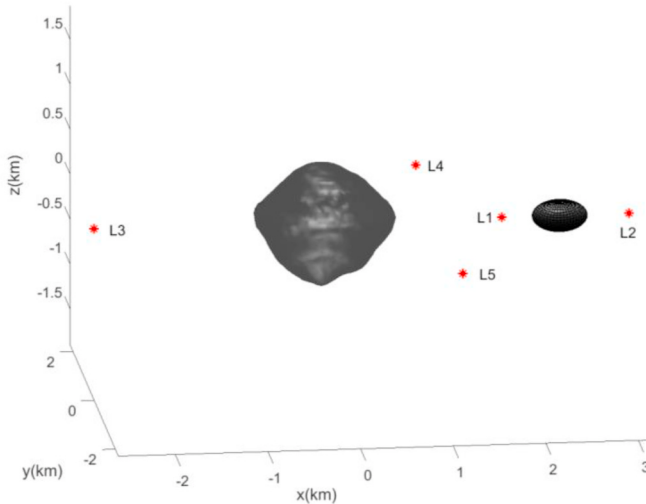


Fig. 3. The five libration points in the gravity field of the nominal binary system.

matrix, and $A(\tau)$ is the Jacobian matrix at time τ , which can be expressed as

$$A(\tau) = \frac{\partial f(X)}{\partial X}(\tau) = \begin{bmatrix} 0 & 0 & 0 & 1 & 0 & 0 \\ 0 & 0 & 0 & 0 & 1 & 0 \\ 0 & 0 & 0 & 0 & 0 & 1 \\ \omega^2 + U_{poly_{xx}} + U_{ell_{xx}} & U_{poly_{xy}} + U_{ell_{xy}} & U_{poly_{xz}} + U_{ell_{xz}} & 0 & 2\omega & 0 \\ U_{poly_{yx}} + U_{ell_{yx}} & \omega^2 + U_{poly_{yy}} + U_{ell_{yy}} & U_{poly_{yz}} + U_{ell_{yz}} & -2\omega & 0 & 0 \\ U_{poly_{zx}} + U_{ell_{zx}} & U_{poly_{zy}} + U_{ell_{zy}} & U_{poly_{zz}} + U_{ell_{zz}} & 0 & 0 & 0 \end{bmatrix} \quad (9)$$

If λ is an eigenvalue of the monodromy matrix, then λ^{-1} , $\bar{\lambda}$, and $\bar{\lambda}^{-1}$ are also eigenvalues of the monodromy matrix. Therefore, the characteristic multipliers of the monodromy matrix can have the following form: 1, -1 , $e^{\pm\alpha}$ ($\alpha \in (0, 1)$), $-e^{\pm\alpha}$ ($\alpha \in (-1, 0)$), $e^{\pm i\beta}$ ($\beta \in (0, \pi)$), and $e^{\pm\sigma\pm i\tau}$ ($\sigma > 0$, $\tau \in (0, \pi)$). Additionally, periodic orbits have at least two characteristic multipliers equal to 1, which can be used to check whether the orbit is periodic.

The topological structures of the submanifolds for the orbits in the gravity field of an irregular body are classified into 34 different cases, including thirteen cases for periodic orbits (Jiang et al., 2015) [23]. The names of the topological structures in Jiang et al. (2015) [23] are adopted in this paper for unification. In our study, only four cases of topological structures are found in libration orbit families: Case P3, Case P4, Case P6, and Case PPD4. These four cases are shown in Fig. 2.

Table 1
Locations of the five libration points of the nominal binary system.

	L1	L2	L3	L4	L5
x(m)	1788.971	3156.609	-2613.179	1112.916	1111.235
y(m)	0.658	0.192	27.747	2224.808	-2224.172
z(m)	0.721	0.117	1.268	0.199	0.759

Table 2
Eigenvalues of the five libration points of the nominal binary system.

	L1	L2	L3	L4	L5
$\lambda_{1,2}(10^{-4})$	± 3.407	± 2.000	± 0.385	$0.214 \pm 0.736i$	$0.214 \pm 0.736i$
$\lambda_{3,4}(10^{-4})$	$\pm 2.617i$	$\pm 1.761i$	$\pm 1.043i$	$-0.214 \pm 0.736i$	$0.214 \pm 0.736i$
$\lambda_{5,6}(10^{-4})$	$\pm 2.602i$	$\pm 1.704i$	$\pm 1.033i$	$\pm 1.008i$	$\pm 1.006i$

Cases P3 and P4 are basic topological structures of libration periodic orbits. These two cases can change to each other through the critical cases, Case P6 and PPD4, with the change characterized as bifurcation. There are four basic kinds of bifurcations of the periodic orbits in the gravity field of irregular-shaped asteroids, including tangent bifurcation, period-doubling bifurcation, real saddle bifurcation, and Neimark–Sacker bifurcation. These four kinds of bifurcations have been found in periodic orbit families around asteroid 216 Kleopatra (Jiang

et al., 2015) [23].

Tangent bifurcation occurs when the characteristic multipliers of the periodic orbit cross 1 and the topological structure of the periodic orbit changes to another case, such as Case P3 → Case P6 → Case P4 or Case P4 → Case P6 → Case P3. In a symmetric system like CR3BP, another bifurcation called pitchfork bifurcation may occur when the characteristic multipliers of the periodic orbit cross 1. The northern and southern halo orbit families both bifurcating from the Lyapunov orbit family at the branching point is a typical pitchfork bifurcation.

Period-doubling bifurcation occurs when the characteristic multipliers of the periodic orbit cross -1 and the topological structure of the periodic orbit changes to another case, such as Case P4 → Case PPD4 → Case P3. In some orbit families, the characteristic multipliers of the periodic orbit cross -1 , but the topological structure of the periodic orbit does not change. This phenomenon is called the pseudo period-

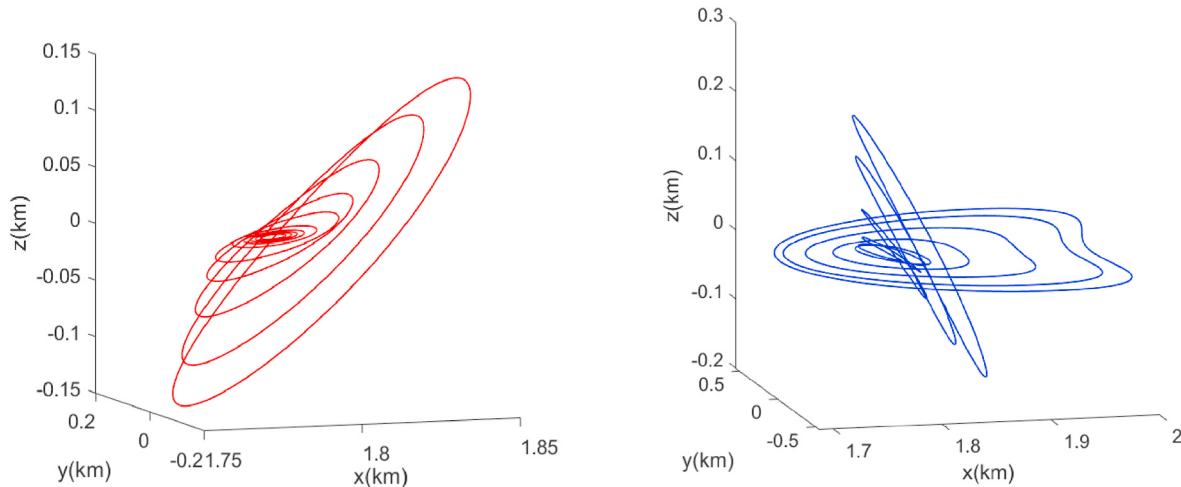


Fig. 4. The southern halo orbit family (red) and the northern halo orbit family (blue) associated with L1 in the nominal binary system. (For interpretation of the references to color in this figure legend, the reader is referred to the Web version of this article.)

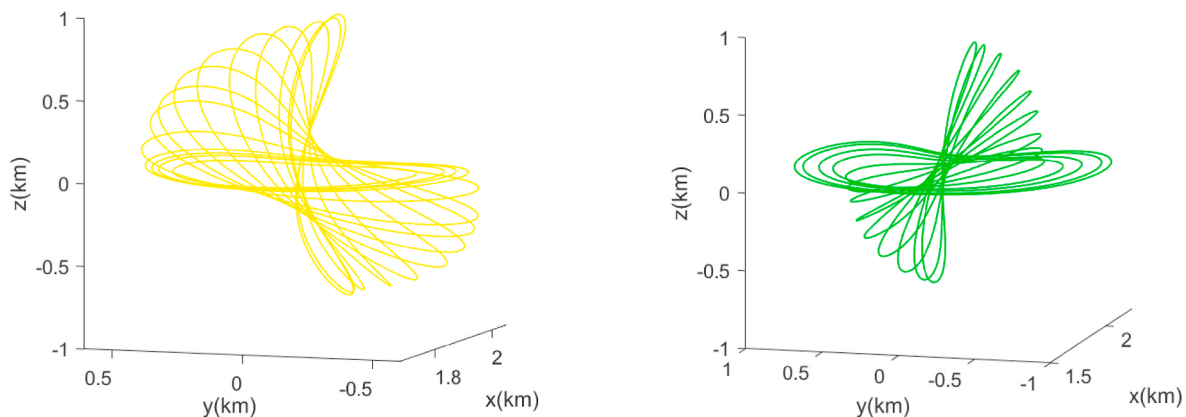


Fig. 5. The axial orbits from the medium Lyapunov orbits (yellow) and the axial orbits from the large Lyapunov orbits (green) associated with L1 in the nominal binary system. (For interpretation of the references to color in this figure legend, the reader is referred to the Web version of this article.)

doubling bifurcation (Jiang et al., 2015) [23].

Real saddle bifurcation occurs when the characteristic multipliers of the periodic orbit cross the real axis and the topological structure of the

periodic orbit changes to another case. Neimark–Sacker bifurcation occurs when the characteristic multipliers of the periodic orbit cross the unit circle without 1 and -1 in the complex plane and the topological structure of the periodic orbit changes to another case.

Since the libration point orbits always have two characteristic multipliers equal to 1 and at least two characteristic multipliers on the real axis, real saddle bifurcation and Neimark–Sacker bifurcation cannot exist in libration orbit families. Actually, only tangent bifurcations have been found in the libration orbit families in this study.

3. Libration points and libration point orbits in the nominal binary system

The binary asteroid system 66391 Moshup is chosen as an example in this study. We use the shape model data from NASA's database (<http://echo.jpl.nasa.gov/asteroids/shapes/>) and physical properties from Ostro et al. (2006) [26]. The distance between the asteroids' centers of mass is 2.55 (km). The semi-axes of the secondary α , β , and γ are 0.297, 0.225, and 0.171 (km), respectively (Scheeres, 2016) [27]. The masses of the primary and the secondary are 2.353 and 0.135 (10^{12} kg), respectively. The density of the primary is 1.97 (g/cm³). The periods of the mutual orbit and the secondary's rotation are both 17.4223 (h).

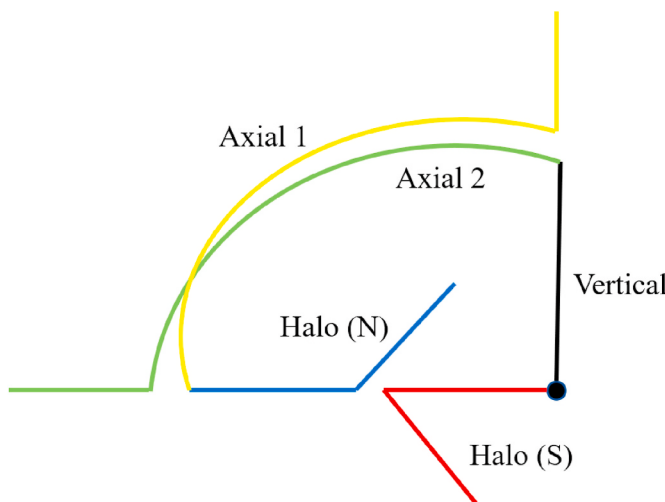


Fig. 6. The connections between libration point orbit families associated with L1 in the nominal binary system.

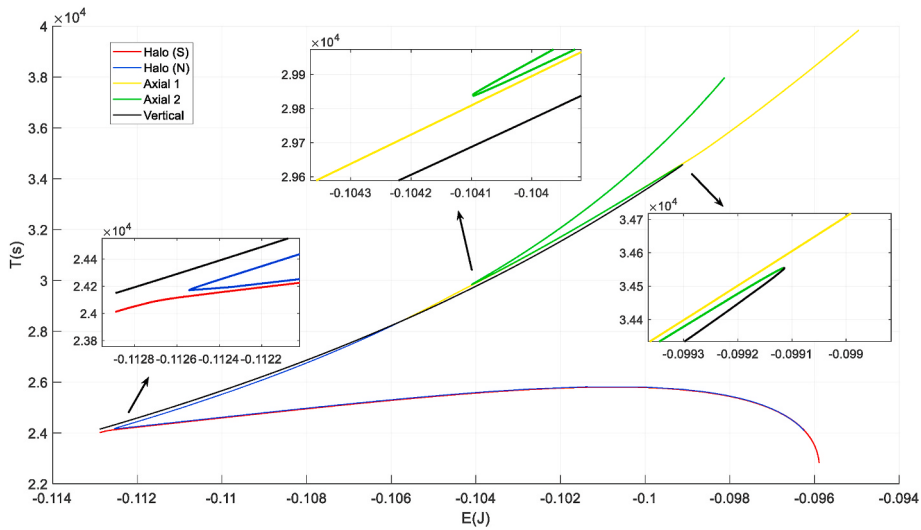


Fig. 7. The energy–period curves of L1 libration point orbit families in the nominal binary system.

3.1. Libration points

Since the motion of the binary system is assumed to be doubly-synchronous, the dynamical system of our RF3BP is autonomous. Equilibrium solutions exist when both the velocity and acceleration are zero, which means

$$f(X) = 0. \quad (10)$$

The locations of the five libration points are shown in Fig. 3, and their coordinates are listed in Table 1. Since the gravity field is asymmetric, the collinear libration points in the CR3BP are not collinear with the primary and secondary in the RF3BP, and the triangular libration points do not form equilateral triangles with the primary and secondary in the RF3BP. Additionally, all five libration points are slightly displaced in the z -direction.

The linear stability of libration points can be determined by the eigenvalues of the Jacobian matrix as expressed in Eq. (9). The largest real part of eigenvalues is defined as

$$\Lambda = \max_{1 \leq i \leq 6} \text{Re}(\lambda_i) \quad (11)$$

where λ_i is the i th eigenvalue of the Jacobian matrix. The libration point is stable, marginally stable, and unstable if $\Lambda < 0$, $\Lambda = 0$, and $\Lambda > 0$, respectively.

The characteristic equation of the Jacobian matrix has the form

$$\lambda^6 + a\lambda^4 + b\lambda^2 + c = 0, \quad (12)$$

where a , b , and c are constants. If λ is an eigenvalue of the matrix, then $-\lambda$, $\bar{\lambda}$, and $-\bar{\lambda}$ are also eigenvalues of the matrix. The eigenvalues of all libration points are listed in Table 2. The topological structures of libration points are the same as those in the CR3BP. All libration points are unstable because $\Lambda > 0$. For L1, L2, and L3, there are two pairs of purely imaginary eigenvalues and one pair of real eigenvalues, indicating that these three libration points have one-dimensional unstable/stable manifolds and four-dimensional center manifolds. For L4 and L5, there are four complex eigenvalues and one pair of purely imaginary eigenvalues, indicating that these two libration points have two-dimensional unstable/stable manifolds and two-dimensional center manifolds.

3.2. Libration point orbits

Libration point orbits have been successfully implemented in deep

space missions since the 1970s and have the potential to be used in future binary asteroids missions. In the CR3BP, both the planar Lyapunov orbit family and the vertical Lyapunov orbit family emanate from L1, L2, and L3 due to the four-dimensional central manifolds of collinear libration points, whereas only the vertical Lyapunov orbit family emanates from L4 and L5 due to the two-dimensional central manifolds of triangular libration points. In the proximity region of the libration points, the periodic orbit families in the RF3BP are similar to those in the CR3BP, because the libration points in the RF3BP have the same topological structural as those in the CR3BP.

For L1, the Lyapunov orbits in the RF3BP have small out of plane components, so they are nearly but not strictly planar. With the increase of orbital energy, the size of the Lyapunov orbit becomes larger, the out of plane components increase, and the orbit family becomes more complicated. The Lyapunov orbit family breaks into three parts that connect to different orbit families. The small Lyapunov orbits emanating from L1 merge with the southern halo orbit family, as shown in Fig. 4 (red). The medium Lyapunov orbits connect the northern halo orbit family and one branch of the axial orbit family (Axial 1), as shown in Fig. 4 (blue) and Fig. 5 (yellow). The large Lyapunov orbits merge with another branch of the axial orbit family (Axial 2), as shown in Fig. 5 (green).

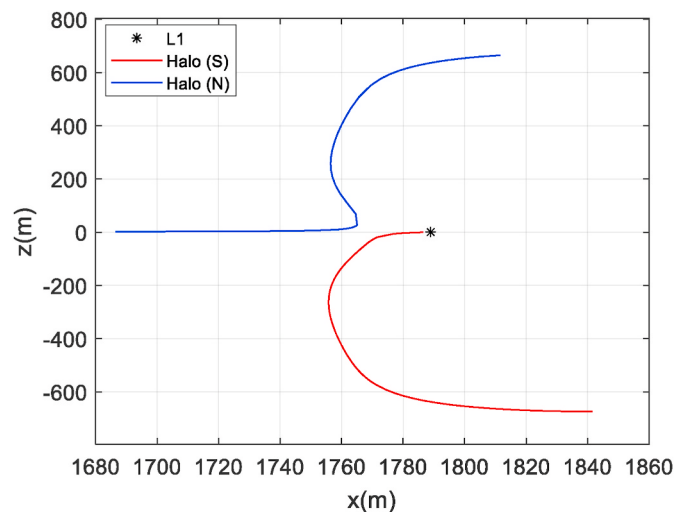


Fig. 8. The northern and southern halo orbit families associated with L1 within the section Σ_0 in the nominal binary system.

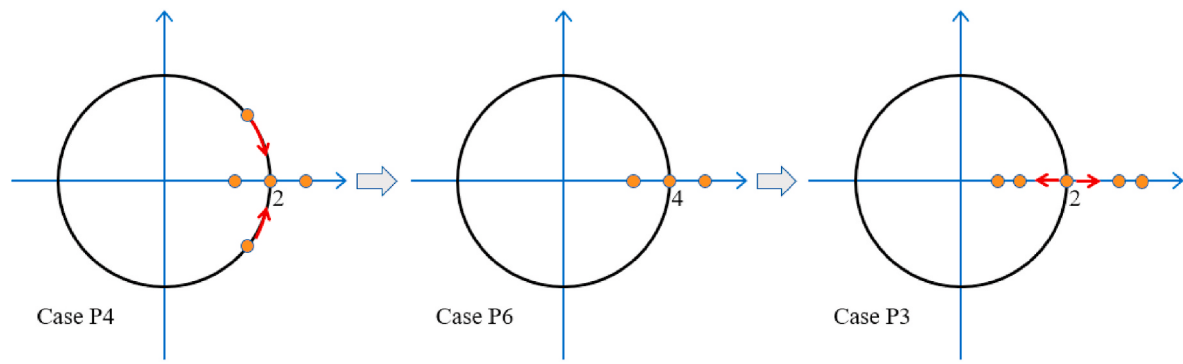


Fig. 9. The topological transition path of the tangent bifurcation in the blue branch of orbit families associated with L1 in the nominal binary system. (For interpretation of the references to color in this figure legend, the reader is referred to the Web version of this article.)

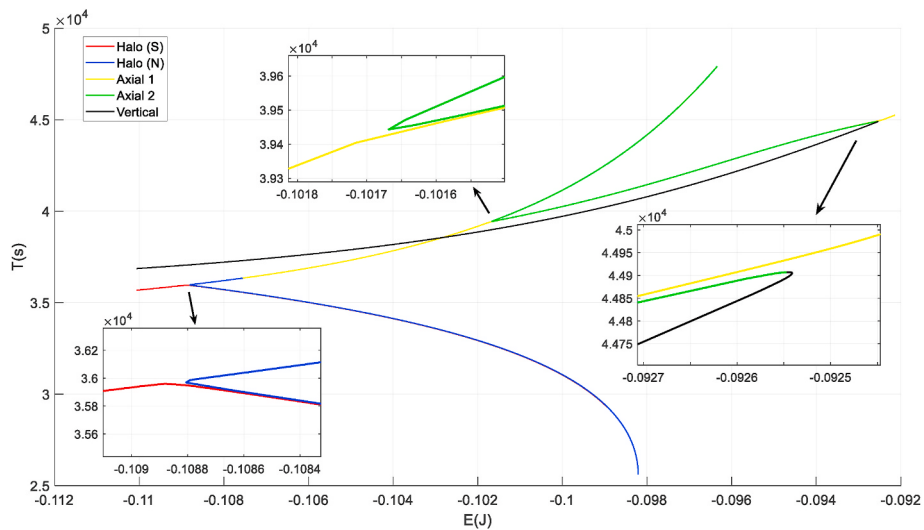


Fig. 10. The energy–period curves of L2 libration point orbit families in the nominal binary system.

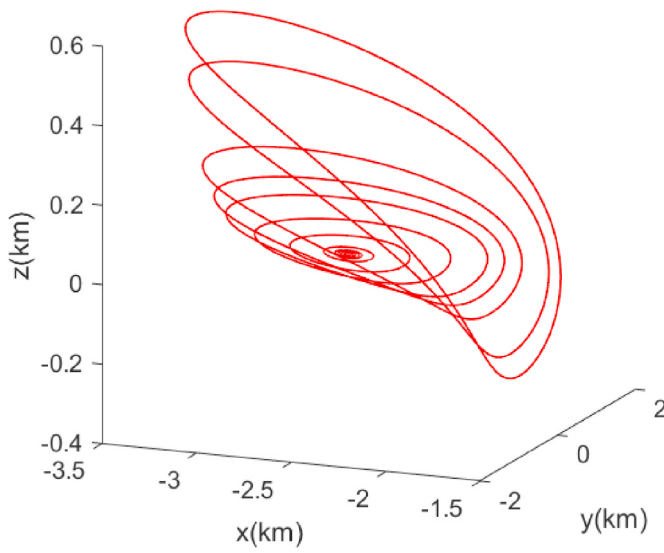


Fig. 11. The northern halo orbit family associated with L3 in the nominal binary system.

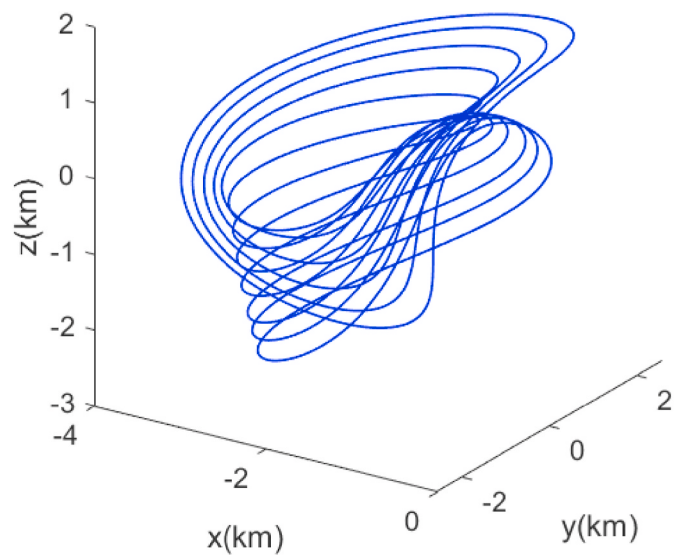


Fig. 12. The southern halo orbit family and the axial orbit family associated with L3 in the nominal binary system.

The axial orbit family in the RF3BP still connects the Lyapunov orbits and the vertical Lyapunov orbits as in the CR3BP. However, there are some differences, because the vertical Lyapunov orbit family breaks into two parts: the small vertical Lyapunov orbits and the large vertical Lyapunov orbits. One branch of the axial orbit family (Axial 1) connects the medium Lyapunov orbits and the large vertical Lyapunov orbits; another branch of the axial orbit family (Axial 2) connects the large Lyapunov orbits and the small vertical Lyapunov orbits. Fig. 6 qualitatively shows the connections between libration point orbit families. The period and energy are important characteristics of an orbit. Fig. 7 shows the energy-period curves of the libration point orbit families associated with L1, which can confirm the connections of these orbit families shown in Fig. 6.

In the CR3BP, the northern and southern halo orbit families both intersect with the Lyapunov orbit family at the same orbit called the branching point. However, the branching point does not exist in the RF3BP, because the northern and southern halo orbit families do not intersect with each other, and they connect to different parts of the Lyapunov orbit family. To quantitatively show the relation of northern and southern halo orbit families, we define a cross section

$$\{\Sigma_0 : y = y_{L1}, y > 0\}$$

where y_{L1} is the y -coordinate of the libration point L1. The intersections of the northern and southern halo orbit families with the section Σ_0 are shown in Fig. 8. Due to the asymmetry of the gravity field, the northern and southern halo orbit families lose symmetry, and no longer connect to each other. This shows that the bifurcation in the Lyapunov orbit family has changed, and the pitchfork bifurcation that gives rise to the halo orbit families in the CR3BP does not exist in the RF3BP. Figs. 7 and 8 are the verifications of the connections between libration point orbit families shown in Fig. 6 from different aspects.

The characteristic multipliers of periodic orbits in the red branch, i.e., small Lyapunov orbits and the southern halo orbit family, cross -1 , but the topological structure of the periodic orbits does not change. Therefore, only the pseudo period-doubling bifurcation occurs in the red branch. In the blue branch, i.e., medium Lyapunov orbits and the northern halo orbit family, the characteristic multipliers of periodic orbits cross 1 , and the topological structure of the periodic orbit changes to another case, implying that a tangent bifurcation occurs in the blue branch. Fig. 9 shows the topological transition path of the tangent bifurcation in the blue branch: Case P4 → Case P6 → Case P3.

There are two pitchfork bifurcations related to the axial orbit family in the CR3BP, the first pitchfork bifurcation occurs when the axial orbit family intersects with the Lyapunov orbit family, and the second

pitchfork bifurcation occur when the axial orbit family intersects with the vertical Lyapunov orbit family. Like the pitchfork bifurcation related to the halo orbit family discussed before, these two pitchfork bifurcations no longer exist either in the RF3BP, and two tangent bifurcations occur as substitutions. The first tangent bifurcation occurs when the large Lyapunov orbits and the axial orbits (Axial 2) intersect in the green branch, and near the second break of the Lyapunov orbit family. The second tangent bifurcation occurs when the vertical Lyapunov orbits and the axial orbits (Axial 1) intersect, and near the break of the vertical Lyapunov orbit family.

The L2 periodic orbit families are analogous to those associated with L1. The connections between libration point orbit families associated with L2 are the same as in the case of L1, and the Lyapunov orbit family and the vertical Lyapunov orbit family also break into three and two parts, respectively. The pitchfork bifurcation does not exist either and the tangent bifurcation occurs as a substitution. The energy-period curves of the libration point orbit families associated with L2 are shown in Fig. 10.

The L3 periodic orbit families have some differences with those associated with L1 and L2. The small Lyapunov orbits merge into the northern halo orbit family, as shown in Fig. 11, and the medium and large Lyapunov orbits do not exist for L3 due to the strong asymmetry of the gravity field of the primary. The southern halo orbit family directly merges with the axial orbit family, as shown in Fig. 12. The energy-period curves of the libration point orbit families associated with L3 are shown in Fig. 13. Compared with the L1 and L2 periodic orbits, the periods show smaller changes with the increase of energy.

Similar to the CR3BP, only the vertical Lyapunov orbit family exists for L4 and L5, as shown in Fig. 14. There is no bifurcation occurring in these families. The energy-period curves of orbit families are shown in Fig. 15.

4. Libration points and periodic orbit families with different shapes of the secondary

The effect of asteroid shape uncertainty needs to be considered in the study of dynamical environments, and the secondary of a binary system usually has higher shape uncertainty than the primary. In this section, variations of libration points and libration point orbit families are investigated with a varying shape of the secondary. The secondary is modelled as an ellipsoid, and its shape is varied by changing the semi-axes, with its mass unchanged in order to maintain the mass ratio of the binary system.

The three semi-axes of the secondary are changed respectively to

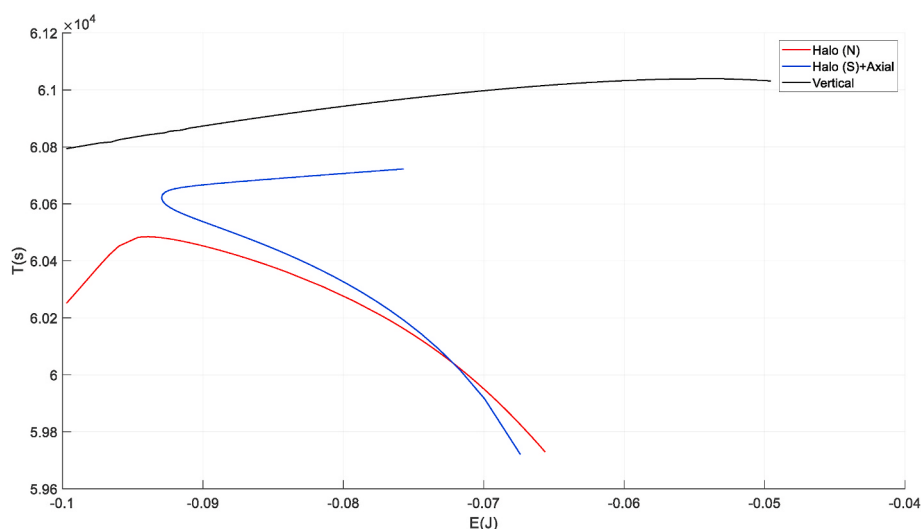


Fig. 13. The energy-period curves of L3 libration point orbit families in the nominal binary system.

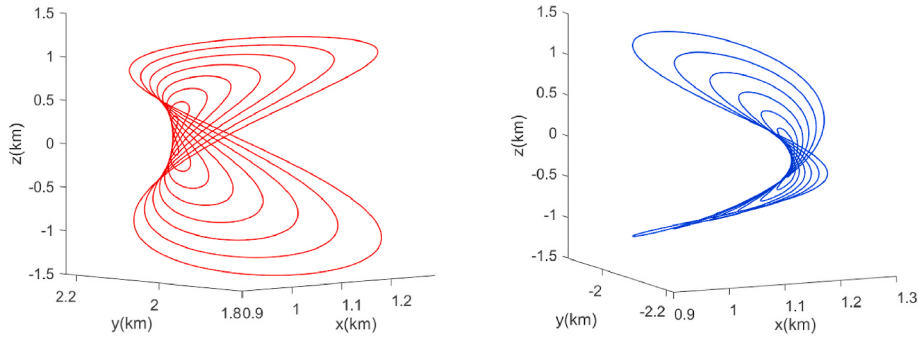


Fig. 14. The L4 (red) and L5 (blue) vertical orbit families in the nominal binary system. (For interpretation of the references to color in this figure legend, the reader is referred to the Web version of this article.)

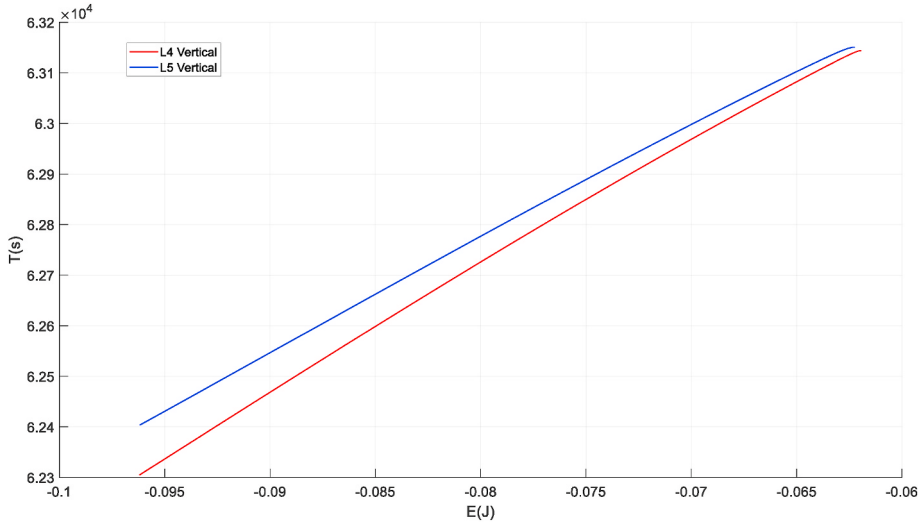


Fig. 15. The energy–period curves of L4 and L5 vertical Lyapunov orbit families in the nominal binary system.

estimate the influence of each. To maintain the long axis equilibria (Bellerose and Scheeres, 2007) [28], the relation of semi-axes, $\alpha \geq \beta \geq \gamma > 0$, needs to be satisfied. Five cases are considered for each semi-axis of the secondary, respectively. The groups A, B, and C represent the cases of changing the semi-axis α , β , and γ , respectively.

4.1. Group A

Five cases are considered in group A: The semi-axis α is changed to 0.8α , 0.9α , 1.1α , and 1.2α , respectively, while the semi-axes β and γ remain unchanged. The positions of five libration points in the different cases are listed in Table 3. As the semi-axis α increases, the libration points L1 and L2 are moving away from the secondary, and the positions of other libration points have barely changed. Among the five libration points, the libration point L1 is the closest to the secondary, so the dynamical environments around L1 are affected most significantly.

Table 3

Positions of the libration points with different values of α .

	0.8 α	0.9 α	α	1.1 α	1.2 α
L1 (m)	(1798.499, 0.677, 0.734)	(1794.026, 0.668, 0.728)	(1788.971, 0.658, 0.721)	(1783.313, 0.647, 0.713)	(1777.031, 0.634, 0.703)
L2 (m)	(3147.271, 0.203, 0.122)	(3151.667, 0.198, 0.119)	(3156.609, 0.192, 0.117)	(3162.106, 0.186, 0.114)	(3168.168, 0.180, 0.111)
L3 (m)	(-2613.170, 27.748, 1.268)	(-2613.174, 27.748, 1.268)	(-2613.179, 27.748, 1.268)	(-2613.184, 27.747, 1.268)	(-2613.189, 27.747, 1.268)
L4 (m)	(1111.935, 2225.279, 0.199)	(1112.398, 2225.057, 0.199)	(1112.916, 2224.808, 0.199)	(1113.490, 2224.532, 0.199)	(1114.121, 2224.228, 0.199)
L5 (m)	(1110.260, -2224.639, 0.758)	(1110.720, -2224.419, 0.759)	(1111.235, -2224.172, 0.759)	(1111.806, -2223.899, 0.759)	(1112.432, -2223.598, 0.759)

Therefore, we focus on the libration point L1 and associated libration point orbits in the rest of this section.

In different cases, the topological structure of libration point L1 remains the same, and the eigenvalues are shown in Table 4. The eigenvalue $\lambda_{3,4}$ and $\lambda_{5,6}$ are essentially related to the in-plane motion (the Lyapunov orbit) and the out-of-plane motion (the vertical Lyapunov orbit), respectively. The connections and bifurcations of periodic orbit families associated with L1 in group A are the same as those in the nominal binary

Table 4

Eigenvalues of the libration point L1 with different values of α .

	0.8 α	0.9 α	α	1.1 α	1.2 α
$\lambda_{1,2}(10^{-4})$	± 3.323	± 3.362	± 3.407	± 3.459	± 3.518
$\lambda_{3,4}(10^{-4})$	$\pm 2.563i$	$\pm 2.588i$	$\pm 2.617i$	$\pm 2.650i$	$\pm 2.687i$
$\lambda_{5,6}(10^{-4})$	$\pm 2.545i$	$\pm 2.571i$	$\pm 2.602i$	$\pm 2.637i$	$\pm 2.677i$

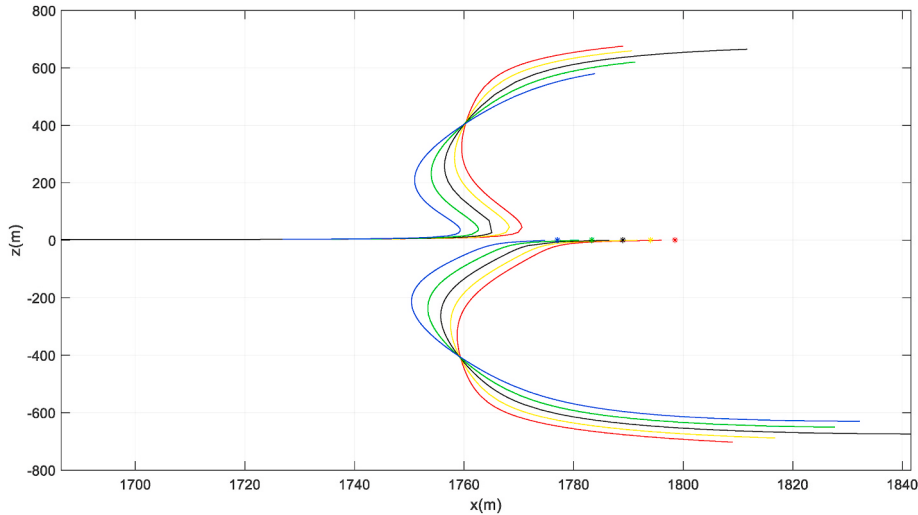


Fig. 16. The northern and southern halo orbit families associated to L1 within the section Σ_0 with different values of α .

system. With the increase of the semi-axis α , the difference between the moduli of eigenvalues $\lambda_{3,4}$ and $\lambda_{5,6}$ becomes smaller, and the first break of the Lyapunov orbit family will appear sooner during the continuation, as shown in Fig. 16. The color red, yellow, black, green, and blue represent the case 0.8α , 0.9α , α , 1.1α , and 1.2α , respectively.

4.2. Group B

In group B, the semi-axis β is changed to 0.8β , 0.9β , 1.1β , and 1.2β , respectively, while the semi-axes α and γ maintain the same. The positions of libration point L1 in different cases are listed in Table 5. As the semi-axis β increases, the libration point L1 is also moving away from the secondary. Compared with the case of changing α , changing β has less effect on the positions of the libration points, but has more

Table 5
Positions of the libration point L1 with different values of β .

	0.8β	0.9β	β	1.1β	1.2β
x(m)	1786.233	1787.534	1788.971	1790.537	1792.226
y(m)	0.644	0.651	0.658	0.666	0.674
z(m)	0.725	0.723	0.721	0.719	0.716

Table 6
Eigenvalues of the libration point L1 with different values of β .

	0.8β	0.9β	β	1.1β	1.2β
$\lambda_{1,2}(10^{-4})$	± 3.434	± 3.421	± 3.407	± 3.393	± 3.377
$\lambda_{3,4}(10^{-4})$	$\pm 2.648i$	$\pm 2.633i$	$\pm 2.617i$	$\pm 2.598i$	$\pm 2.580i$
$\lambda_{5,6}(10^{-4})$	$\pm 2.605i$	$\pm 2.603i$	$\pm 2.602i$	$\pm 2.601i$	$\pm 2.599i$

significant effect on the eigenvalues of the libration point L1. The eigenvalues of libration point L1 in different cases are listed in Table 6.

As the semi-axis β decreases from the nominal value to 0.8β , the connections between orbit families and bifurcations are the same as those in the nominal binary system. But as the semi-axis β increases to 1.1β , the moduli of eigenvalue $\lambda_{5,6}$ become greater than those of eigenvalue $\lambda_{3,4}$, indicating that the period of the vertical Lyapunov orbit is smaller than the period of the Lyapunov orbit in the neighborhood of the libration point L1.

Another extraordinary result in case 1.1β is that the halo orbit families bifurcate from the vertical Lyapunov orbit family instead of the Lyapunov orbit family, which was also discovered by Scheeres et al. [22] in the Mars-Phobos system. The northern and southern halo orbits are shown in Fig. 17. The axial orbit family also bifurcates from the vertical Lyapunov orbit family, as shown in Fig. 18. Therefore, the connections between libration point orbit families in the case 1.1β are different from the results in the nominal binary system and the cases in group A.

Fig. 19 qualitatively shows the connections between the libration point orbit families associated with L1, and the energy-period curves of the libration point orbit families associated with L1 are shown in Fig. 20. There is no break and bifurcation in the Lyapunov orbit family, which is represented by the black curves in Figs. 19 and 20. But the vertical Lyapunov orbit family breaks into four parts. The first part merges with the southern halo orbit family, which is represented by the red curves in Figs. 19 and 20. For the blue curves in Figs. 19 and 20, the second part of the vertical Lyapunov orbit family connects the northern halo orbit family and one branch of the axial orbit family (Axial 1), and this branch of axial orbit family also connects to the fourth part of the vertical Lyapunov orbit family. Fig. 21 shows that the third part of the vertical

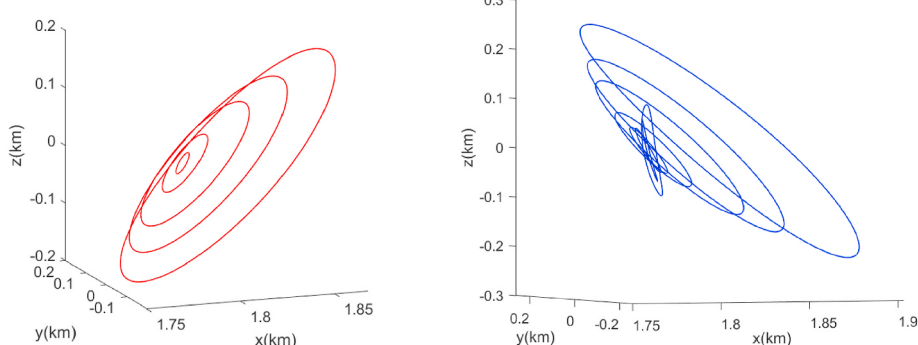


Fig. 17. The northern and southern halo orbits associated with L1 in the case of 1.1β .

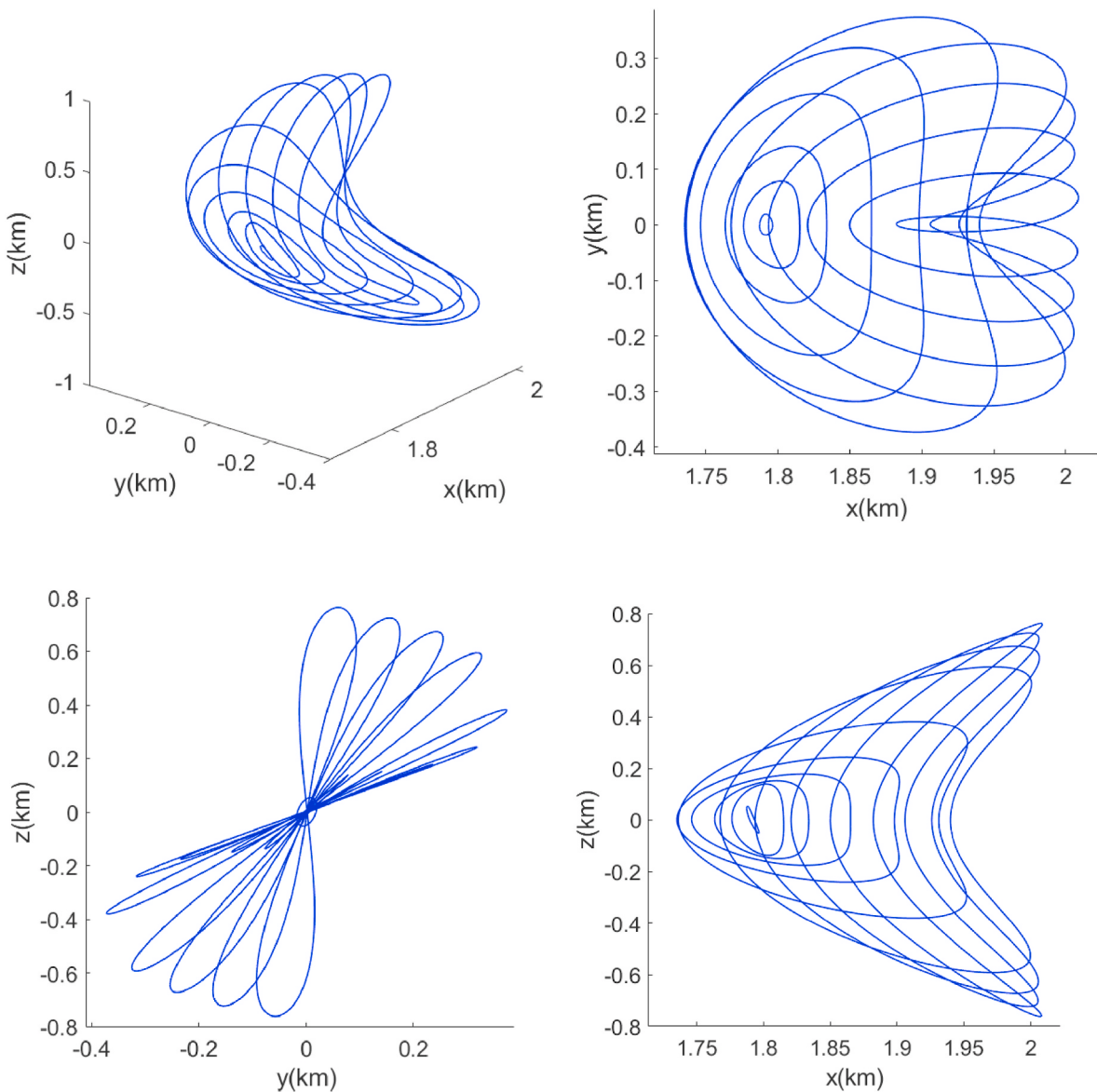


Fig. 18. One branch of the axial orbit family (Axial 1) associated with L1 in the case of 1.1β .

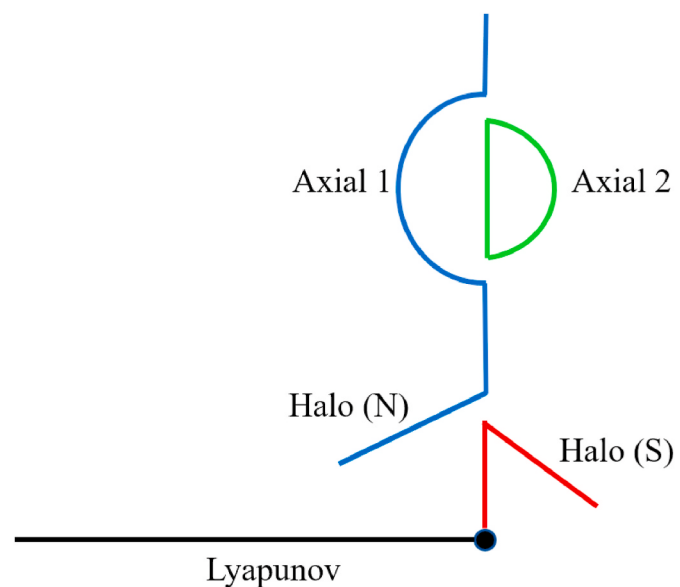


Fig. 19. The connections between the L1 orbit families in the case of 1.1β .
25

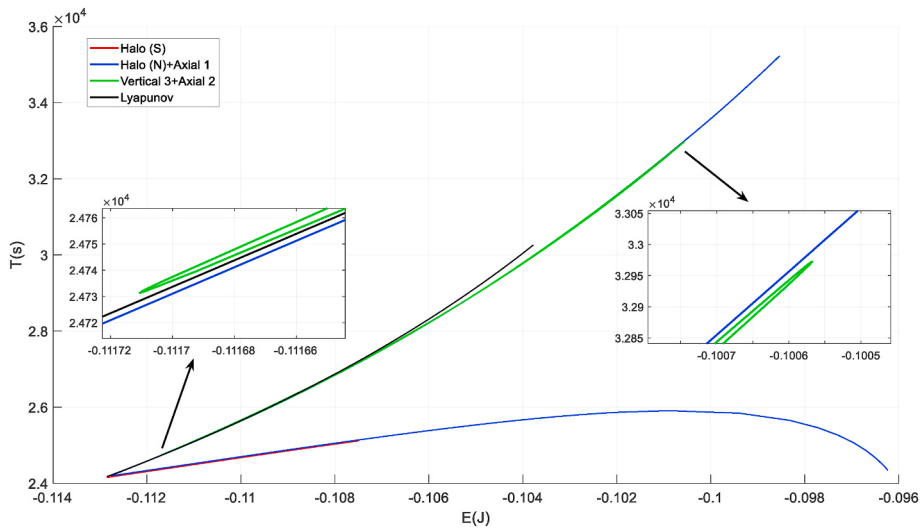


Fig. 20. The energy–period curves of L1 orbit families in the case of 1.1β .

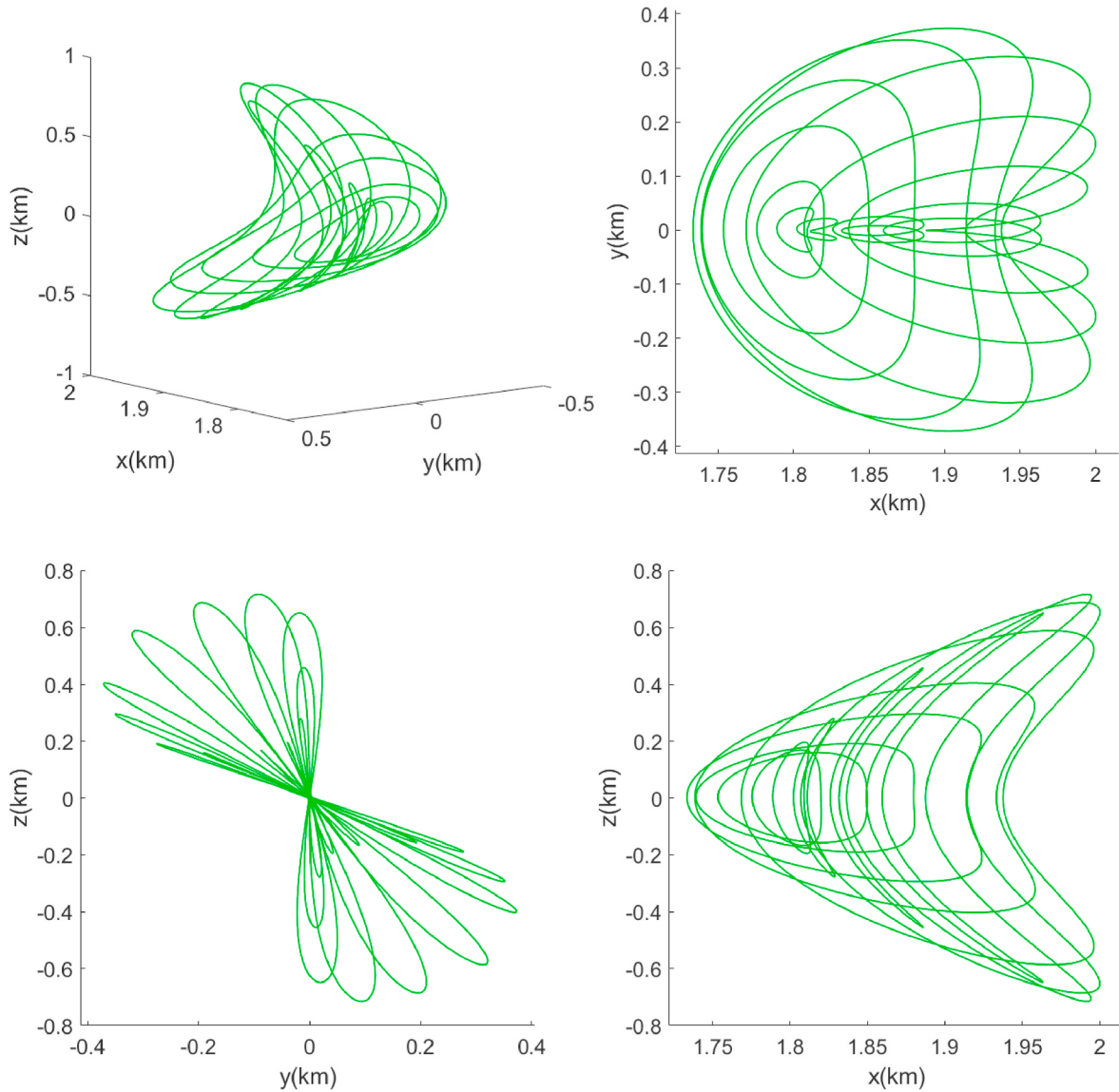


Fig. 21. The orbit cycle constructed by the third part of the vertical Lyapunov orbits and another branch of the axial orbit family (Axial 2) associated with L1 in the case of 1.1β .

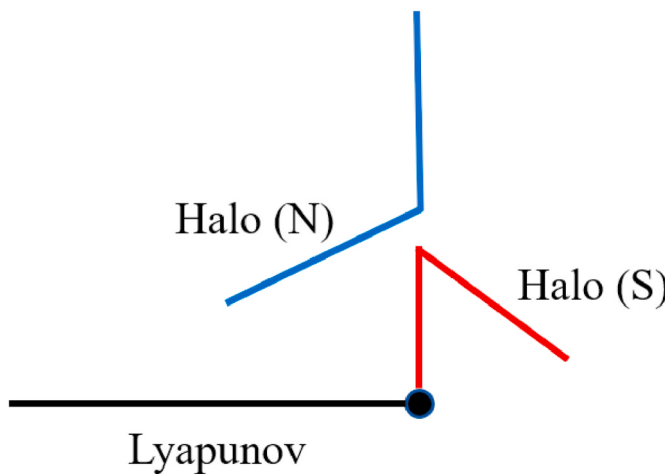


Fig. 22. The connections between the L1 orbit families in the case of 1.2β .

Lyapunov orbit family connects with another branch of the axial orbit family (Axial 2) at both ends, constructing a cycle (the green curves in Figs. 19 and 20). So, the axial orbit family does not connect the Lyapunov orbit family and the vertical Lyapunov orbit family, but connects with only the vertical Lyapunov orbit family at both ends.

The bifurcations of periodic orbits are similar to those in the nominal binary system: One tangent bifurcation occurs in one branch of orbits near each breakpoint. Binary tangent bifurcations occur in the orbit cycle, and the topological transition path is Case P4 → Case P6 → Case P3 → Case P6 → Case P4.

When the semi-axis β increases to 1.2β , the halo orbit families also bifurcate from the vertical Lyapunov orbit family, but the axial orbit family is not found during the continuations of the Lyapunov orbit family and the vertical Lyapunov orbit family. So, the vertical Lyapunov orbit family breaks into only two parts, and the small part and the large part merge with the southern and northern halo orbits, respectively. Fig. 22 qualitatively shows the connections between the libration point

Table 7

Positions of the libration point L1 with different values of γ .

	0.8γ	0.9γ	γ	1.1γ	1.2γ
x(m)	1787.325	1788.106	1788.971	1789.919	1790.948
y(m)	0.659	0.659	0.658	0.657	0.656
z(m)	0.714	0.717	0.721	0.725	0.729

Table 8

Eigenvalues of the libration point L1 with different values of γ .

	0.8γ	0.9γ	γ	1.1γ	1.2γ
$\lambda_{1,2}(10^{-4})$	± 3.422	± 3.415	± 3.407	± 3.399	± 3.390
$\lambda_{3,4}(10^{-4})$	$\pm 2.617i$	$\pm 2.617i$	$\pm 2.617i$	$\pm 2.616i$	$\pm 2.616i$
$\lambda_{5,6}(10^{-4})$	$\pm 2.620i$	$\pm 2.611i$	$\pm 2.602i$	$\pm 2.592i$	$\pm 2.581i$

orbit families associated with L1, and the energy-period curves of the libration orbit families associated with L1 are shown in Fig. 23. The same color in Figs. 22 and 23 represent the same orbit family.

4.3. Group C

In group C, the semi-axis γ is changed to 0.8γ , 0.9γ , 1.1γ , and 1.2γ , respectively, while the semi-axes α and β remain unchanged. The positions of libration point L1 in different cases are listed in Table 7. Compared with the cases of changing α and β , changing γ has the same effect on the positions of the libration points, but a different effect on eigenvalues of the libration point L1. As the semi-axis γ increases, the eigenvalues $\lambda_{3,4}$ barely change, and the moduli of eigenvalues $\lambda_{5,6}$ decrease. The eigenvalues of the libration point L1 in different cases are listed in Table 8.

When the semi-axis γ changes to 0.9γ , 1.1γ , or 1.2γ , the connections between orbit families and bifurcations of periodic orbits are the same as those in the nominal binary system. But when the semi-axis γ decreases to 0.8γ , the moduli of eigenvalue $\lambda_{5,6}$ become greater than those of the eigenvalue $\lambda_{3,4}$, and the connections between orbit families and

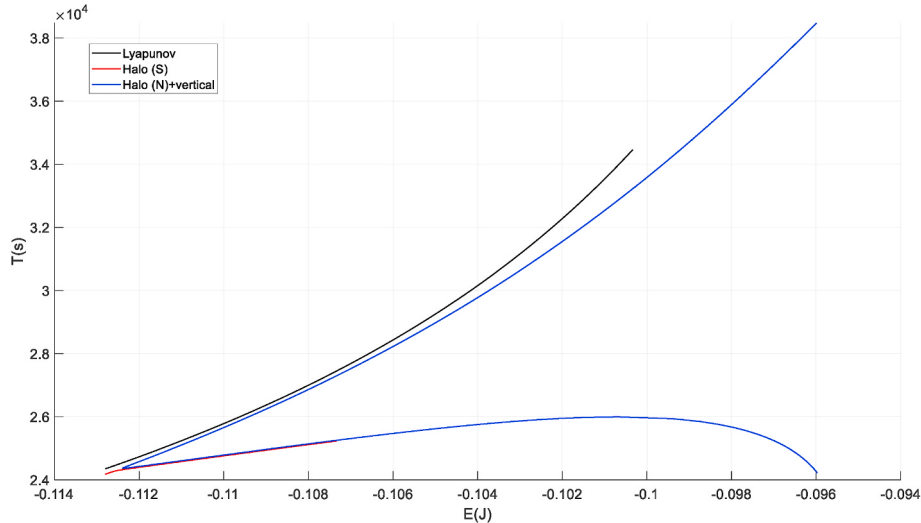


Fig. 23. The energy-period curves of the L1 orbit families in the case of 1.2β .

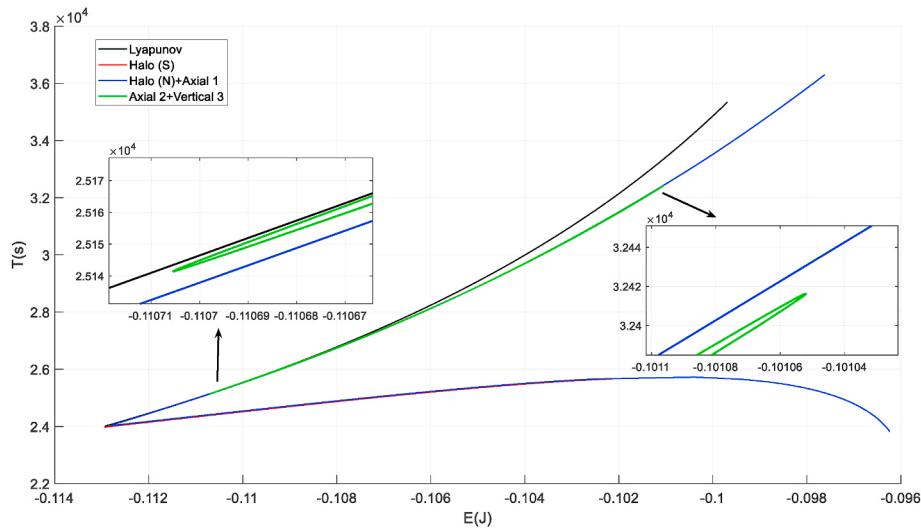


Fig. 24. The energy–period curves of the L1 orbit families in the case of 0.8γ .

bifurcations of periodic orbits are similar to those in the case of 1.1β . The energy–period curves of the libration point orbit families associated with L1 in the case of 0.8γ are shown in Fig. 24.

5. Conclusion

With the primary modelled as a polyhedron and the secondary modelled as a triaxial ellipsoid, libration points and associated periodic orbit families in the gravity field of a binary asteroid system, as well as their variations with different shapes of the secondary, have been investigated numerically.

In the case of the nominal binary system, the five libration points have the same topological structures as those in the CR3BP. However, all libration points have been displaced slightly due to the irregular shapes of the asteroids. The connections between libration point orbit families are different from those in the CR3BP. For L1 and L2, the Lyapunov orbit family breaks into three parts, and the vertical Lyapunov orbit family breaks into two parts. The southern and northern halo orbits lose symmetry and connect with small and medium Lyapunov orbits, respectively. The two branches of axial orbits also lose symmetry, one branch of which connects the medium Lyapunov orbits and the large vertical Lyapunov orbits, and another branch of which connects the large Lyapunov orbits and the small vertical Lyapunov orbits. For L3, the Lyapunov orbit family exists only in the small region near the libration point, and merges with the northern halo orbits. The southern halo orbits directly merge with the axial orbit family. These results indicate that the pitchfork bifurcations that give rise to halo orbit families and the axial orbit family in the CR3BP do not exist in the RF3BP, and the tangent bifurcation occurs as a substitution.

Then, the shape of the secondary was varied by changing the semi-axes, and libration points and associated periodic orbit families were investigated accordingly. The results have shown that changing α has the most significant effect on position offsets of the libration points, while changing β has the most significant effect on eigenvalues of the libration points. When the moduli of the eigenvalue $\lambda_{5,6}$ are greater than those of $\lambda_{3,4}$, the halo orbit families and the axial orbit family will bifurcate from the vertical Lyapunov orbit family instead of the Lyapunov orbit family. For example, in the cases of 1.1β and 0.8γ , the connections between orbit families are different from those in the nominal binary system. There is no breakpoint in the Lyapunov orbit family, but the vertical Lyapunov orbit family breaks into four parts: the first part merges with the southern halo orbit family; the second part connects the northern halo orbit family and one branch of the axial orbit family, which also connects the fourth part; the third part connects

another branch of the axial orbit family at both ends. In the case of 1.2β , the halo orbit families also bifurcate from the vertical Lyapunov orbit family, but the axial orbit family has not been found. The vertical Lyapunov orbit family breaks into only two parts, and the small part and the large part merge with southern and northern halo orbits, respectively.

Although only the binary asteroid system 66391 Moshup is considered, the methods are applicable to other binary systems, and the results provide general insights into the dynamical environments in the proximity of binary asteroid systems. The results indicate that the periodic orbit families in the irregular gravity field are much more complicated than those in the CR3BP, and changing the semi-axes of the secondary has significant effects on connections between libration point orbit families. The shape uncertainty of the primary may also have significant effects on the libration points and the periodic orbit families, which needs to be investigated by changing the primary's shape in the future.

Declaration of competing interest

The authors declare that they do not have any commercial or associative interest that represents a conflict of interest in connection with the paper submitted.

Acknowledgments

This work has been supported by the National Natural Science Foundation of China under Grants 11872007, the Advanced Study Program by the Chinese Academy of Sciences (Grant No. CSU-QZKT-2019-05), the Young Elite Scientist Sponsorship Program by China Association for Science and Technology under Grant 2017QNRC001, and the Fundamental Research Funds for the Central Universities.

References

- [1] J.L. Margot, M. Nolan, L. Benner, S. Ostro, R. Jurgens, J. Giorgini, M.A. Slade, D. B. Campbell, Binary asteroids in the near-earth object population, *Science* 296 (5572) (2002) 1445–1448.
- [2] M. Čuk, D. Nesvorný, Orbital evolution of small binary asteroids, *Icarus* 207 (2010) 732–743.
- [3] D.J. Scheeres, J. Bellerose, The restricted Hill full 4-body problem: application to spacecraft motion about binary asteroids, *Dyn. Syst. Int. J.* 20 (1) (2005) 23–44.
- [4] D.J. Scheeres, Dynamics about uniformly rotating triaxial ellipsoids: applications to asteroids, *Icarus* 110 (2) (1994) 225–238.
- [5] R.A. Werner, D.J. Scheeres, Exterior gravitation of a polyhedron derived and compared with harmonic and mascon gravitation representations of asteroid 4769 Castalia, *Celestial Mech. Dyn. Astron.* 65 (3) (1996) 313–344.

- [6] J. Bellerose, D.J. Scheeres, Periodic orbits in the vicinity of the equilateral points of the restricted full three-body problem, in: AAS/AIAA Conference, Lake Tahoe, California, AAS-05-295, vol. 711, 2005.
- [7] J. Bellerose, D. Scheeres, General dynamics in the restricted full three body problem, *Acta Astronaut.* 62 (10) (2008) 563–576.
- [8] J. Bellerose, D.J. Scheeres, Restricted full three-body problem: application to binary system 1999 KW4, *J. Guid. Contr. Dynam.* 31 (1) (2008) 162–171.
- [9] L. Chappaz, K.C. Howell, Exploration of bounded motion near binary systems comprised of small irregular bodies, *Celestial Mech. Dyn. Astron.* 123 (2) (2015) 123–149.
- [10] P. Woo, A.K. Misra, Bounded trajectories of a spacecraft near an equilibrium point of a binary asteroid system, *Acta Astronaut.* 110 (2015) 313–323.
- [11] X. Xin, X. Hou, Equilibrium points in the restricted full three body problem with ellipsoidal primaries, *Astron. J.* 154 (1) (2017) 37.
- [12] X. Hou, X. Xin, A note on the full two-body problem and related restricted full three-body problem, *Astrodynamicas* 2 (1) (2018) 39–52.
- [13] X. Li, D. Qiao, M.A. Barucci, Analysis of equilibria in the doubly synchronous binary asteroid systems concerned with non-spherical shape, *Astrodynamicas* 2 (2) (2018) 133–146.
- [14] X. Li, D. Qiao, P. Li, Bounded trajectory design and self-adaptive maintenance control near non-synchronized binary systems comprised of small irregular bodies, *Acta Astronaut.* 152 (2018) 768–781.
- [15] Y. Shi, Y. Wang, S. Xu, Equilibrium points and associated periodic orbits in the gravity of binary asteroid systems:(66391) 1999 KW4 as an example, *Celestial Mech. Dyn. Astron.* 130 (4) (2018) 32.
- [16] L. Dell'elce, N. Baresi, S.P. Naidu, L.A. Benner, D.J. Scheeres, Numerical investigation of the dynamical environment of 65803 Didymos, *Adv. Space Res.* 59 (5) (2017) 1304–1320.
- [17] A. Capannolo, F. Ferrari, M. Lavagna, Families of bounded orbits near binary asteroid 65803 Didymos, *J. Guid. Contr. Dynam.* 42 (1) (2018) 189–198.
- [18] P. Woo, A.K. Misra, Equilibrium points in the full three-body problem, *Acta Astronaut.* 99 (2014) 158–165.
- [19] G. Gómez, J.M. Mondelo, The dynamics around the collinear equilibrium points of the RTBP, *Physica D* 157 (4) (2001) 283–321.
- [20] W.S. Koon, M.W. Lo, J.E. Marsden, S.D. Ross, *Dynamical Systems, the Three-Body Problem and Space Mission Design*, Marsden Books, Wellington, 2008.
- [21] L. Chappaz, K. Howell, Trajectory exploration within binary systems comprised of small irregular bodies, in: 23rd AAS/AIAA Space Flight Mechanics Meeting, Kauai, Hawaii, 2013.
- [22] D.J. Scheeres, S. Van wal, Z. Olikara, N. Baresi, Dynamics in the phobos environment, *Adv. Space Res.* 63 (1) (2019) 476–495.
- [23] Y. Jiang, Y. Yu, H. Baoyin, Topological classifications and bifurcations of periodic orbits in the potential field of highly irregular-shaped celestial bodies, *Nonlinear Dynam.* 81 (1–2) (2015) 119–140.
- [24] Y. Ni, Y. Jiang, H. Baoyin, Multiple bifurcations in the periodic orbit around Eros, *Astrophys. Space Sci.* 361 (5) (2016) 170.
- [25] J.M.A. Danby, *Fundamentals of Celestial Mechanics*, second ed., Willmann–Bell, Richmond, VA, 1992, pp. 102–111.
- [26] S.J. Ostro, J.L. Margot, L.A. Benner, J.D. Giorgini, D.J. Scheeres, E.G. Fahnestock, et al., Radar imaging of binary near-earth asteroid (66391) 1999 KW4, *Science* 314 (5803) (2006) 1276–1280.
- [27] D.J. Scheeres, *Orbital Motion in Strongly Perturbed Environments: Applications to Asteroid, Comet and Planetary Satellite orbiters*, Springer, 2016.
- [28] J. Bellerose, D.J. Scheeres, Stability of libration points in the restricted full three-body problem, *Acta Astronaut.* 60 (3) (2007) 141–152.